Indonesian Geotechnical Journal, August 2025, Vol 4 (2). Page 99-112
DOI: https://doi.org/10.56144/igj.v4i2.120
EISSN: 2829-7520
https://indonesian-geotechnical-journal.org/index.php/JGI/issue/archive

Effectiveness of buttress wall in reducing wall deflection for deep excavation supported by tied-back retaining wall systems

Ari Surya Abdi[1],*, Muhammad Dwiyanto Agung Prakasa[2]
[1]Department of Civil Engineering, National Taiwan University, No. 1, Section 4, Roosevelt Road, Da'an District, Taipei City, 10617, Taiwan; arisuryaabdi.asa@gmail.com
[2]Department of Civil Engineering, State Polytechnic of Ujung Pandang, Makassar, 90245, Indonesia; dwiyantoagung@poliupg.ac.id
*Correspondence: arisuryaabdi.asa@gmail.com

SUBMITTED 21 July 2025 **REVISED** 27 July 2025 **ACCEPTED** 30 August 2025

ABSTRACT This study evaluates the effectiveness of buttress walls (BWs) in reducing wall deflection and ground anchor force in deep excavations supported by tied-back retaining systems. A three-dimensional finite element model (3D FEM) was employed for the study. First, a well-documented excavation project located in Vietnam that adopted BW in combination with ground anchors was first back-analyzed to validate the numerical model. The results showed good agreement between computed wall deflections and field measurements across all excavation stages. In the Vietnam case study, the BW was temporary and was demolished after the final excavation stage. The ground anchors installed were to limit the wall deflection during BW demolition. Parametric studies were then conducted to assess two BW configurations: inner BW (I-BW), placed within the excavation area (Vietnam case), and outer BW (O-BW), located behind the retaining wall. The two configurations were analyzed with and without ground anchors. In addition, one run with only ground anchors was conducted to evaluate the effectiveness of BW vs. ground anchors. Results show that both BW configurations reduced wall deflections and anchor forces, with O-BW performing slightly better in the absence of ground anchors due to additional frictional resistance between the BW and the retained soil throughout excavation stages. When ground anchors are used, the difference in performance between I-BW and O-BW becomes negligible due to increased system stiffness. For wall retained by ground anchors only, the deflection of wall is flexible, whilst wall retained by BW only shows rigid behaviour. The maximum deflection, however, is of similar magnitude when the wall is retained by O-BW only and ground anchors only. The deflection is slightly larger when retained by I-BW only. The findings highlight the potential of combining BWs with anchors to increase the rigidity of structural system and enhance excavation safety, particularly under complex soil conditions.

KEYWORDS Deep excavation; Buttress wall; Ground anchor; Wall deflection; Finite element method

1 INTRODUCTION

Deep excavations are essential for urban development, enabling the construction of underground infrastructure such as basements, metro stations, and utility tunnels (Abdi et al. 2025; Abdi and Ou 2023a; Bryson and Zapata-Medina 2012; Lim et al. 2020). In densely populated areas, these excavations often take place in close proximity to existing buildings and facilities, making deformation control a critical aspect of design and safety (Ou et al. 2020; Schuster et al. 2009). Excessive wall deflections can lead to ground movements, structural instability, and potential damage to nearby structures (Abdi 2024; Abdi et al. 2024; Abdi & Ou 2022; Zheng et al. 2022). To mitigate these risks, various stabilization methods have been adopted. Among them, ground anchors and buttress walls (BWs) have been widely used due to their capacity to provide additional lateral resistance and minimize wall movements during excavation (Abdi & Ou 2023b; Hsieh & Ou 2018; Lim et al. 2016, 2018).

For deep excavation with a tied-back retaining system, ground anchors perform by transferring the lateral loads from the retaining wall to the surrounding soil or rock mass, thereby reducing the bending moment and deflection of the wall (Finno & Roboski 2005). On the other hand, the BW

system, typically constructed perpendicular to the main retaining wall, acts as a lateral support system by providing additional frictional resistance and enhancing the overall system's stiffness (Abdi et al. 2025; Hsieh et al. 2016; Hsieh & Ou 2018; Lim et al. 2016, 2020; Ou et al. 2006). By combining these systems, ground anchors and BWs could potentially control wall deflections and reduce structural force, especially in complex geotechnical conditions such as colluvial soils.

Despite the practical application of BWs in conjunction with anchored excavations, there is limited research on their mechanism in controlling wall deflections and structural forces in the literature, particularly in colluvial ground conditions. Most existing studies focus on conventional support systems without examining the role of BWs in a comprehensive manner. In this study, a three-dimensional finite element method (3D FEM) is employed to simulate the performance of a tied-back excavation system with ground anchors and BWs. The model is initially validated against field data from a case study in Vietnam, ensuring its reliability. Subsequently, a series of parametric analyses are conducted to investigate the influence of various BW configurations on wall deflections and anchor forces, providing insights for optimizing excavation support design in challenging soil conditions.

2 VALIDATION OF NUMERICAL MODELLING

2.1 Project Background

The validation of the model was carried out using a well-documented case reported by Bui et al (2024). It was a 22-storeys building constructed using the top-down construction method and the 24.1 m deep excavation was retained by a 26-meter-high diaphragm wall (DW) surrounding the structure on the east, west, and north sides. As the project was located in an urban area, the buttress wall (BW) system was adopted to limit the wall deflection and prevent damage to the adjacent buildings. The BW system was originally designed to be preserved and act as an integral part of the building's structural framework. However, due to aesthetic considerations for the hotel development, the BW system had to be demolished during excavation. To compensate for the BW removal while controlling the deflection during demolition, an anchor system was adopted as an additional support for the DW. The northern wall section is chosen for the investigation in this study, mainly because of its considerable length and close location to crucial infrastructure such as roadways, buried cable systems, drainage infrastructures, and densely populated residential zones.

Eight boreholes as depicted in Figure 1a were drilled to depths between 41 m and 50 m to elucidate the geological conditions of the study area. The boreholes yield data regarding the stratigraphy of soil layers. Standard penetration test (SPT) was conducted during the drilling process, with a distance of 2 m between each test. Soil and rock samples, both disturbed and undisturbed, were tested in the laboratory to discover their physical characteristics and particle composition. Mechanical properties were assessed through the oedometer test, direct shear test, and triaxial test. According to the geological investigations, the soil layer in this project area can be classified mainly into 5 layers excluding the filling soil as shown in Figure 1b. The subsurface profile comprised a complex and heterogeneous sequence of soil layers resulting from erosion, transport, and accumulation of transient flows. The uppermost layer consisted of backfill, commonly found in most boreholes, with an average thickness of 3 m. This layer was composed of a mixture of yellow-grey to yellow-brown clay, gravel, boulders, and concrete. A layer of hard plastic to very stiff clay with gravels was found beneath, ranging from 1.2 to 9.6 m in thickness, having SPT-N values between 7 and 38. A very stiff to hard clay layer mixed with gravel followed, with thickness ranging from 3.4 to 19.0 m and SPT-N values between 11 and 62. A highly weathered grey to dark grey siltstone layer was encountered below, showing a thickness of 1.4 to 5.2 m and SPT-N values between 32 and 50. A subsequent layer consists of clay mixed with successive grits, was located beneath, with a thickness ranging from 3.8 to 5.5 meters and SPT-N values between 8 and 19. The deepest identified layer consisted of a highly weathered sandstone, exhibiting an SPT-N value greater than 50. A more detailed discussion on the soil condition can be referred to the previous study (Bui et al. 2024).

The diaphragm wall thickness was 0.6 m with a depth of 26 m. The compressive strength of the DW concrete ($f'c$) was 25 MPa. The toe of the DW was embedded approximately 5 meters into the weathered sandstone layer with N-SPT value > 50, designated as the hard stratum. Under these conditions, no stability issues were expected. The BWs were constructed subsequent to the completion of the primary DW. Similar to the DW, the thickness and the strength of the BWs are 0.6 m and 25 MPa, respectively. The dimension of BW was 3.2 m in length and 22.25 m in depth, and the BW spacing is approximately 11.7 m. There were two supporting slabs with 0.2 m thickness and 25 MPa of compressive strength employed in this project. They were constructed after the first and second stages of excavation, respectively. Ground anchors were structured into five layers, each with specified lengths as illustrated in Figure 1a. The horizontal and vertical spacing of the ground anchors were 3.2 m and 4.0 m, respectively. The complete cross-sectional excavation profile and ground conditions of this case are depicted in Figure 1b. A monitoring system consisting of 12 inclinometers were installed to monitor the DW movements. The locations of the inclinometers are shown in Figure 1a (DN1-DN12). Monitoring point DN1 was set up for the observation of the DW in the eastern region. Monitoring points DN2-DN7 were installed to observe the lateral deflection of the DW in the northern area, whereas points DN8-DN12 were assigned for monitoring displacements in the western area. In addition to the diaphragm wall monitoring, the anchor forces at four locations were also monitored using four anchor points (load cell). One anchor in the northern region (L4-N2-30) and three anchors (L4-N2-46, L3-N2-45, L1-N2-38) in the transition between northern and eastern regions were monitored. The locations of the monitored anchors are also shown in Figure 1a.

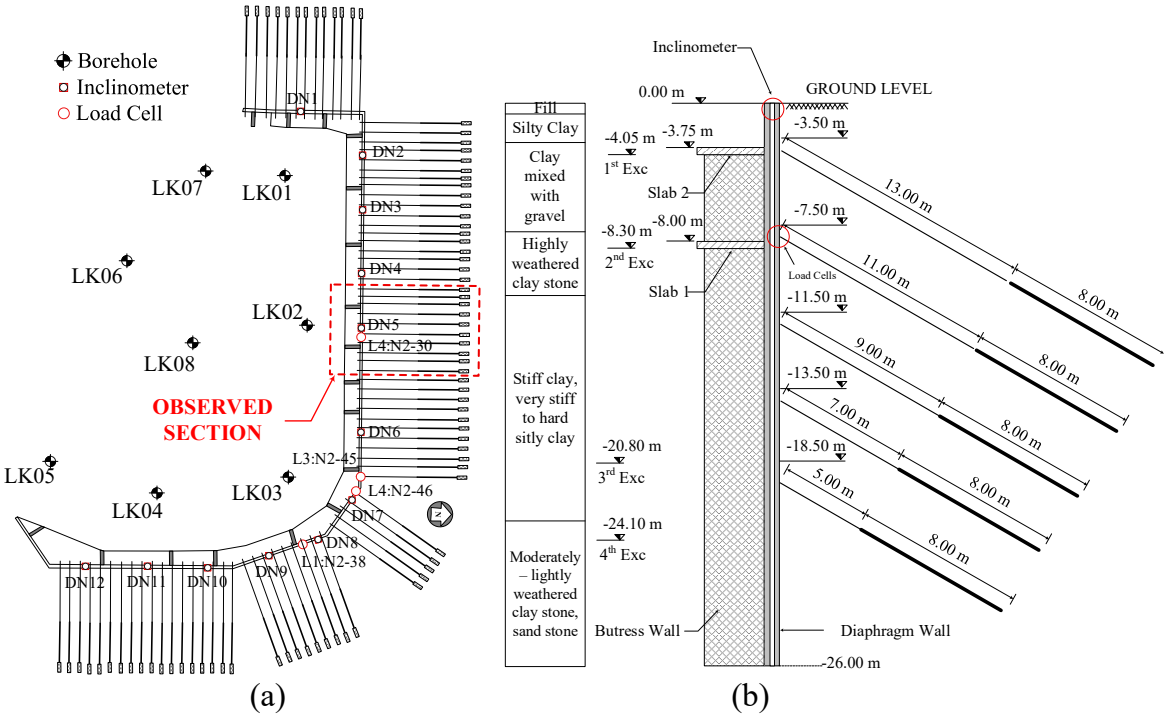

Figure 1. Excavation profile of the Vietnam excavation case: (a) Layout of the installed instrumentations and observed section; (b) Cross-sectional excavation profile and ground condition

2.2 Finite Element Modeling

In this analysis, the three-dimensional (3D) finite element analysis of the northern DW was performed using PLAXIS 3D(Brinkgreve et al. 2021). Figure 2 shows the 3D numerical model used. In order to simplify the analysis, the study will simulate only the section at monitoring location DN5 and L4-N2-30 as shown in Figure 1a. The boundary in the x-direction was 102.30 m, and the distance between the DW and the outer boundary of the mesh was set to be three times the final excavation depth ($3H_e$). This is to reduce the boundary effect in the horizontal direction behind the wall. The width analysed was 20 meters to represent the observed section. The mesh quality was set to be very fine, resulting in a model with 56626 elements.

To represent a more realistic soil behavior, the hardening soil (HS) model was chosen as the constitutive model (Schanz et al. 1999). In the HS model, it is known that there are three types of soil stiffness, which are reference secant stiffness (E_{50}^{ref}), the reference for primary oedometer loading (E_{oed}^{ref}), and the reference unloading-reloading stiffness (E_{ur}^{ref}). The term "reference" in this context denotes the reference stress (the default reference stress is p_{ref} = 100 kPa). The filling soil and weathered stone were simulated as drained material, and the clay layers were simulated as undrained material. As mentioned by Bui et al. (2024), the E_{oed}^{ref} value was derived based on unconfined compression test results. Subsequently, the other stiffnesses, such as reference secant stiffness and reference unloading-reloading stiffness, was obtained using the empirical solution by $E_{oed}^{ref} = E_{50}^{ref}$ and $E_{ur}^{ref} = 3E_{50}^{ref}$ (Calvello & Finno 2004; Schanz et al. 1999). The reported SPT-N value for the deepest layer exceeds 50. According to the studies by (Hsiung et al. 2018) the E_{oed}^{ref} value is typically within the range of 2000 – 4000N (kPa). Therefore, for this layer, the E_{oed}^{ref} value is assumed to be 2500N with SPT-N = 80. For the strength parameters, it was obtained from the triaxial tests (excluding the filling soil layer and the deepest layer, which are assumed). For the dilatancy angle (ψ'), it can be estimated by $\psi' = \varphi' - 30^{o}$ (Brinkgreve et al. 2021; Bolton 1986). The soil parameters utilized for analysis are presented in Table 1.

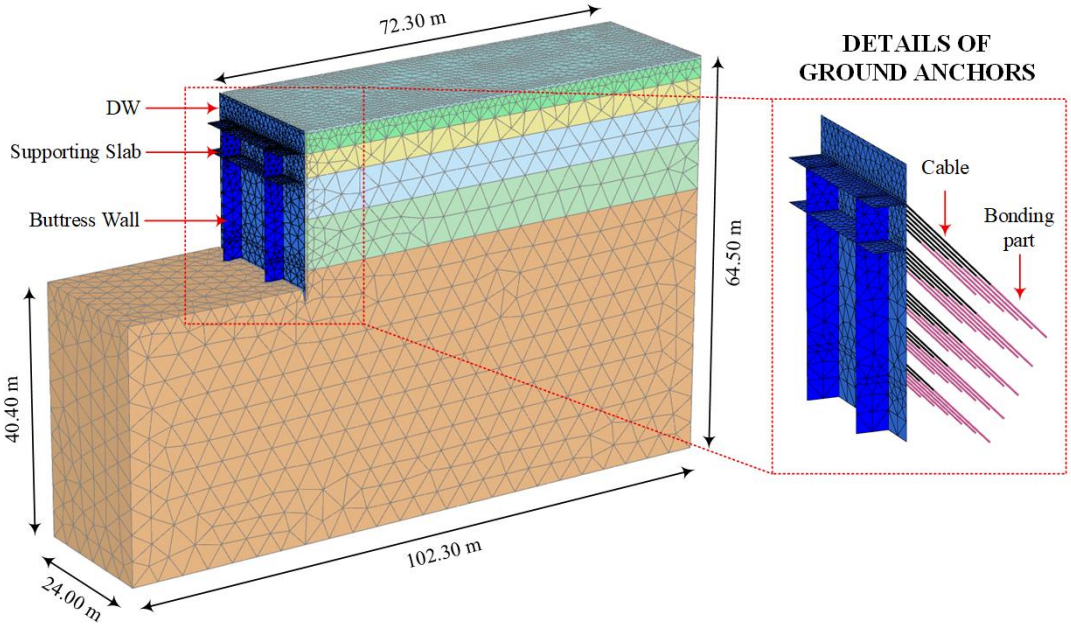

Figure 2. 3D Finite element mesh used in the analysis.

Table 1. Soil parameters used in the analysis

Soil Layer	Filling Soil	Silty Clay	Clay mixed with gravel	Weathered Clay Stone	Hard Silty Clay	Weathered Sandstone
Thickness (m)	0.5	3	3.7	6.3	7.9	43.1
Depth (m)	0.0-0.5	0.5-3.5	3.5-7.2	7.2-13.5	13.5-21.4	21.4-64.5
Drainage type	Drained	Undrained A	Undrained A	Drained	Undrained A	Drained
γ (kN/m^3)	17.5	20.4	20.2	20.9	20.7	26.9
N-SPT	7	22.5	36.5	40	38.5	> 50
E_{50}^{ref} (kN/m^2)	10,000	18,330	17,740	27,110	24,370	200,000
E_{oed}^{ref} (kN/m^2)	10,000	18,330	17,740	27,110	24,370	200,000
E_{ur}^{ref} (kN/m^2)	30,000	54,990	53,220	81,330	73,110	600,000
m	1	1	1	1	1	0.5
c' (kN/m^2)	5	18.7	27.5	30.9	31.3	160
φ' (^{o})	25	29.8	39.6	35.9	37.5	35
ψ' (^{o})	-	-	-	5.9	7.5	5
υ_{ur}	0.2	0.2	0.2	0.2	0.2	0.2
R_{inter}	0.7	0.7	0.7	1	1	1

All the structural elements, DW, BW, and slabs, were modelled using plate elements, and all the input parameters of these structural materials are listed in Table 2. The Young's modulus of concrete (E_c) was estimated according to the standards provided by the American Concrete Institute (ACI 1995), and a reduction factor of 0.8 is adopted considering the crack due to large bending moment (Lim et al. 2016). In order to simulate the soil-structure interaction between the structural objects and soil, the interface elements (R_{inter}) were employed in this model. The R_{inter} used in this model (Table 1) was in the range of 0.7 to 1.0, depending on the type of soil, as suggested by Teng et al (2023). The ground anchors consisted of two parts, which are bonding part and cable. The bonding part was modelled as embedded beam, and the cable was modelled as node-to-node anchor. The prestressed force on the ground anchors were 210 kN and were applied to the node-to-node anchor. The details of ground anchor parameters are listed in Table 3. The numerical procedure followed the sequential construction stages that reflects the actual excavation and construction stages in the field. The numerical procedure is summarized in Table 4.

Table 2. Input parameters of structural elements (Bui et al., 2024)

Structure	Material model	d (m)	E_c (kPa)	υ
Diaphragm wall	Elastic	0.6	2.65×10^7	0.2
Buttress wall	Elastic	0.6	2.65×10^7	0.2
Supporting slab	Elastic	0.3	2.65×10^7	0.2

Table 3. Details of ground anchor parameters

Element	Material type	EA (m)	E (kPa)	D (m)
Bonding part	Elastic	-	3.25×10^7	0.16
Cable	Elastic	7.90×10^4	-	-

Table 4. Construction sequence of the Vietnam's excavation case

Phase	Construction stages
0	Initial Phase
1	Installation of diaphragm wall
2	1st stage of excavation to -4.05 m
3	Construction buttress wall and slab 1
4	2nd stage of excavation to -8.30 m
5	Construction slab 2
6	3rd stage of excavation to -20.80 m
7	Installation of the ground anchor system
8	4th stage of excavation to -24.10 m
9	Dismantled buttress wall (from -4.05 m to -24.10 m)

3 VALIDATION RESULTS

3.1 Wall Deflection After 4th Stage of Excavation (Phase 8)

Figure 3 presents the comparison between the field-measured and numerically computed wall deflections for the Vietnam deep excavation case at the final excavation stage. At the initial stages (stages 1 and 2), the computed wall deflection slightly underestimate the field measurements but had good agreement with the field measurements for stages 3 and 4. The underestimation may be due to the surcharge load from heavy construction equipment at the site worker at stage 1 and 2 or complex soil behavior near the ground surface, which was not considered in the analysis. Nevertheless, both the computed deflection profiles are generally similar to those of the field measurement. The computed wall deflection and field measurements showed a typical linear cantilever shape in all stages. This was due to the rigid system stiffness that was established from the combination of the ground anchors and BW. The maximum horizontal wall deflection (denoted as δ_{hm}) occurred near the top of the DW in both field measurement and numerical results for all stages. Specifically, the FEM simulation produced a δ_{hm} of 63.32 mm at the final stage (stage 4), while the field measurement recorded a closely matching value of δ_{hm} = 62.04 mm. This minimal deviation and similarity in

deflection shape indicates an excellent agreement between the numerical prediction and field measurement, implying that the FEM model has been validated and can further be used to perform parametric studies to investigate the influence of BW configurations on wall deflection and ground anchor forces.

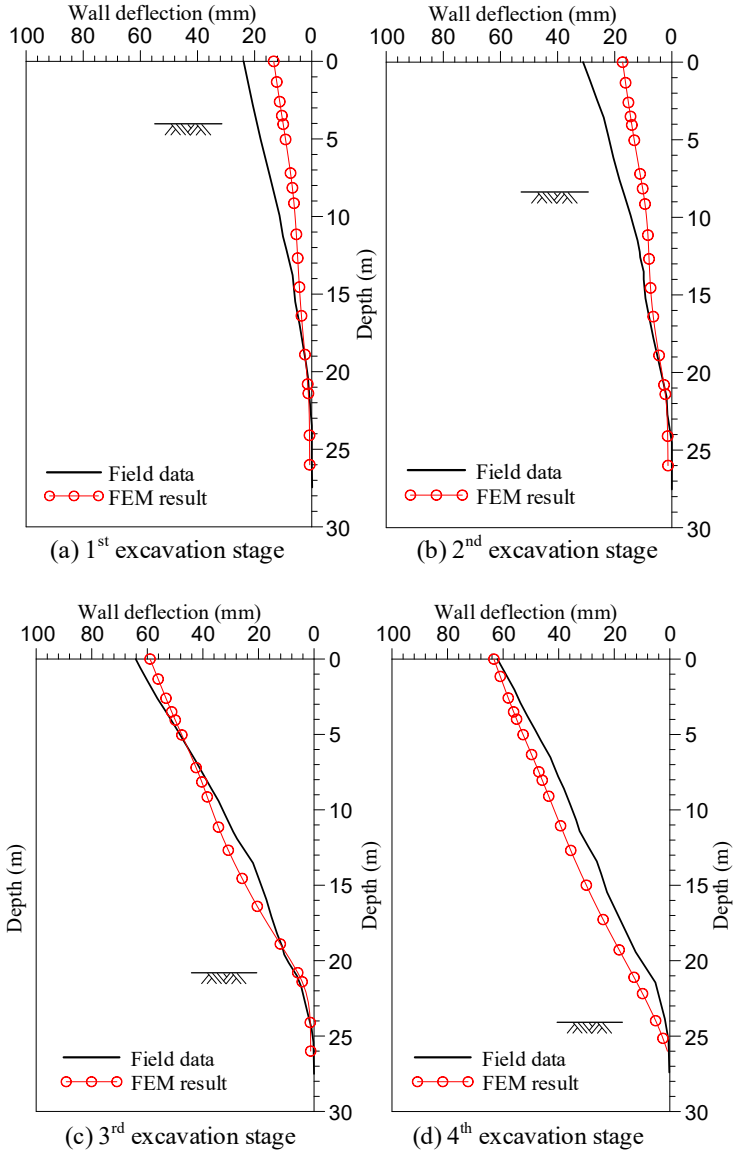

Figure 3. Comparison of field measurements and computed wall deflections for the Vietnam excavation case in all excavation stages.

3.2 Effects of BW Demolition (Phase 9)

This section evaluates the effects of BW demolition after the final excavation stage on the wall deflection and ground anchor forces. Unfortunately, there is no field measurement on the wall deflection after BW demolition. As shown in Figure 4a, the wall deflection slightly increased in the middle of the DW after the BW was demolished. However, the maximum wall deflection, which occurred at the top of DW did not increase as the deflection was resisted by the additional ground anchors. This can be observed by the ground anchor force before and after BW demolition (see Figure 4b). After the BW demolition, there was an increase in ground anchor forces at all levels except for level 1. This is because the wall deflection in this level remained relatively similar even after the demolition. These results indicate that the ground anchors could effectively support and control DW deflection during the BW demolition. Figure 4c shows the development of force in

second level ground anchor across 280 days of monitoring. Unfortunately, it was not specified when the BW demolition began or completed. Different from the numerical results, the ground anchor force reduced with time, from around 230 kN on day 0 to less than 220 kN after 280 days. This might be because of stress relaxation that occurred in the ground anchor, which cannot be captured in the numerical analysis. As there is no data available to cross-check the wall deflection after BW demolition, the effects of this ground anchors relaxation cannot be further investigated. However, the authors believe that the numerical results are sensible, demolition of BW would result in increased wall deflection and increased ground anchor force.

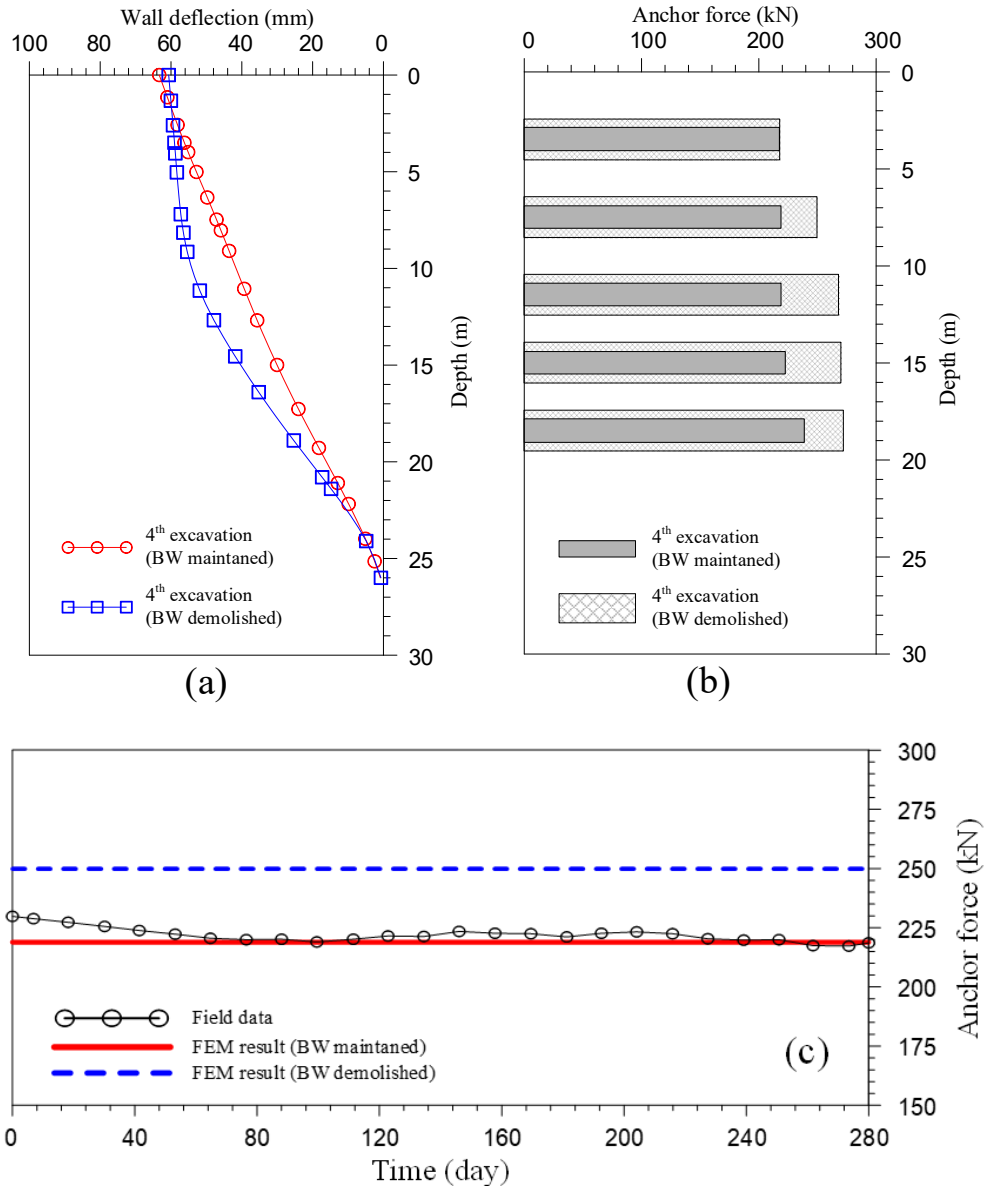

Figure 4. Comparison of numerical results for different BW condition (maintain and demolish) at final excavation stage: (a) wall deflection; (b) ground anchor force; (c) comparison with field measurement of second level ground anchor.

4 PARAMETRIC STUDY ON THE PERFORMANCE OF BW USING DIFFERENT CONFIGURATIONS

In this section, parametric studies considering different BW configurations were conducted to evaluate the effects of BW configuration on the wall deflection and ground anchor forces. According to Lim et al. (2018), there are two possible types of BW, such as inner buttress wall (I-BW) and outer buttress wall (O-BW), which are investigated in this parametric study. Figure 5 illustrates the

configuration of I-BW and O-BW. The I-BW type refers to a buttress wall installed inside the excavation area, whereas the O-BW type is positioned behind the retaining wall. Note that the BW dimensions and spacing are assumed to be the same as those mentioned in the preceding section, i.e., width, length, height and spacing of 0.6 m, 3.2 m, 22.25 m and 11.7 m respectively. In addition to the BW configuration, this paper also investigates the DW performance with and without ground anchors. In total, 5 numerical runs were conducted as tabulated in Table 5.

Table 5. List of numerical runs

Run no.	I-BW	O-BW	With anchor
1. I-BW with anchor	✓		✓
2. I-BW no anchor	✓		
3. O-BW with anchor		✓	✓
4. O-BW no anchor		✓	
5. Anchor only			✓

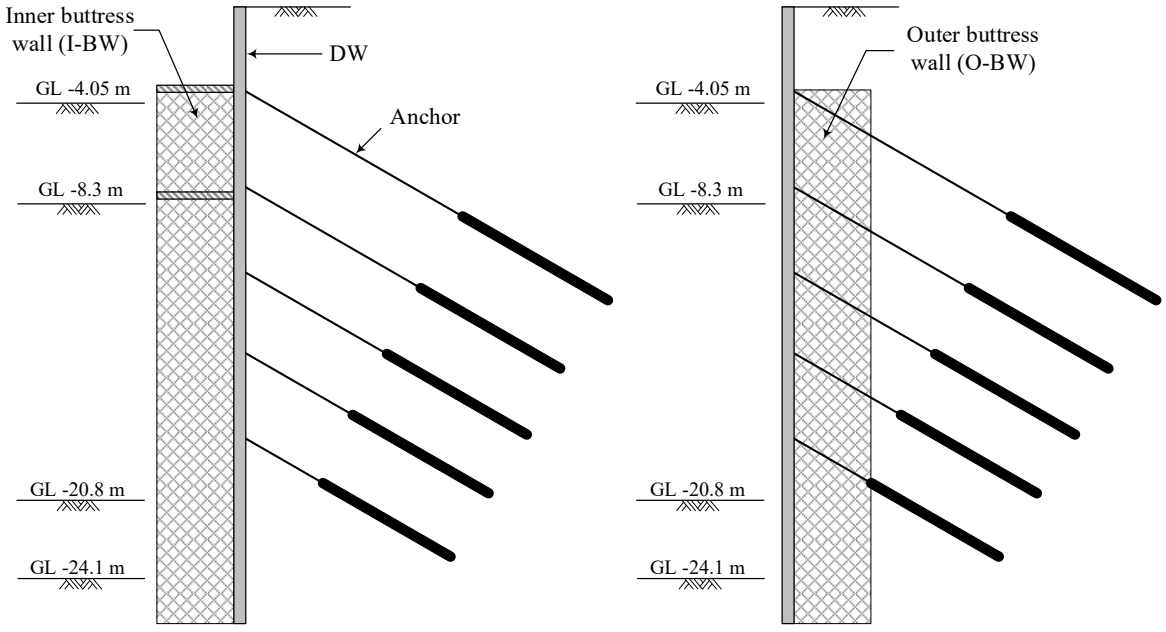

(a) Excavation with I-BW (b) Excavation with O-BW

Figure 5. Schematics diagram of excavation with I-BW and O-BW

Figure 6 shows the computed outputs of the parametric study at the final excavation stage . An obvious observation is that the wall deflection is minimum when both BW and ground anchors are installed. When both BW and ground anchors are installed, the wall deflection profile and magnitude are almost identical regardless of whether the BW is installed inside or outside (δ_{hm} = 63.32 mm for I-BW and δ_{hm} = 62.50 mm for O-BW). When the excavation is done with BW but no anchors, significant increase in deflection can be seen, but less pronounced when the BW is installed in the outer side (δ_{hm} for I-BW = 92.66 mm; δ_{hm} for O-BW = 82.07 mm). This is due to the additional frictional resistance acting on the two sides of BW for the case of O-BW, which is absent in I-BW when the soil is excavated. In the case of ground anchor only (note: anchor without I-BW or O-BW is identical case), the deflection profile changes to be flexible type (non-linier), and the maximum deflection does not occur at the top of DW but somewhere around 6 m depth, slightly above the second excavation.

With only ground anchors, the maximum deflection is lower than I-BW only. However, the lower deflection is only true from the top of DW until 4 m depth, the depth which the I-BW starts. This

implies that the BW rigidity is superior to ground anchors in reducing deflection. If the deflection of the top of DW wants to be reduced, the BW can be constructed up to the ground surface. On the other hand, the maximum deflection of ground anchor only system is similar to that of O-BW. Similar to I-BW, the upper part of DW (up to 3 m depth) reinforced by O-BW deflects slightly more than the ground anchor only system. From all the results, it can be drawn that a combination of BW and ground anchors are effective in reducing wall deflection during excavation. However, if one were to choose among I-BW, O-BW or ground anchors, O-BW is more superior for the case analyzed.

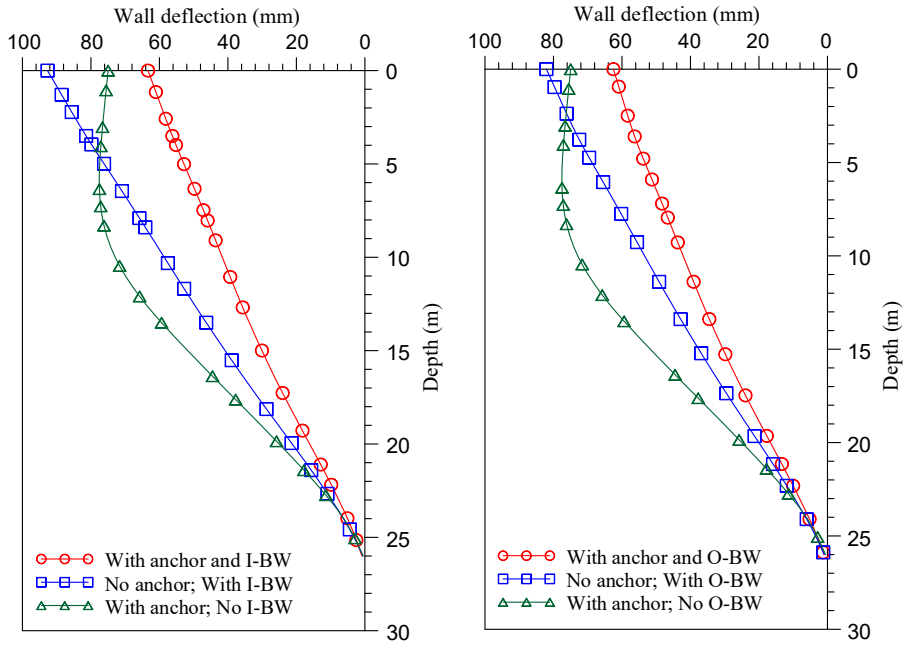

(a) Excavation with I-BW (b) Excavation with O-BW

Figure 6. Comparison of computed wall deflections for inner and outer buttress walls (I-BW and O-BW) varied by different supporting system conditions

In order to further evaluate the performance of I-BW and O-BW in reducing wall deflection, the relative shear stress along the BW surface is investigated. The relative shear stress (τ_{rel}) on the BW interface is defined as:

$$\tau_{rel} = \frac{\tau_{mobilized}}{\tau_{max}} = \frac{\sqrt{\tau_1^2 + \tau_2^2}}{\tau_{max}} \quad (1)$$

where τ_1 and τ_2 is the horizontal and vertical shear stress respectively at any given point on the soil-structure interface, while τ_{max} is the maximum shear stress that dependent on the stress state on that given point. This implies that the frictional resistance on BWs has been fully mobilized when the relative shear stress is equal to unity (τ_{rel} = 1), which also indicates that the permanent slip has occurred. The main source of the vertical frictional resistance was the relative displacement between BWs and the soil heave inside the excavation, while the horizontal frictional resistance was generated by the relative displacement between BWs and adjacent soils due to the lateral wall deflection.

Figure 7 shows the relative shear stress along the BW surface for the I-BW case at different excavation stages. During the 2nd excavation stage, a larger mobilized area was found near the excavation level as compared to the area near the wall toe. This is because a larger wall deflection occurred at the top level (cantilever shape). The frictional resistance is further mobilized for deeper excavation stages, where the friction is almost fully mobilized on all BW surfaces at the final excavation stage. In this stage, the BW has very slight frictional resistance because permanent slip has occurred. Meanwhile, for the case with O-BW, the frictional resistance area remains the same

for all excavation stages, and not all areas are fully mobilized at the final excavation stage and can still provide additional frictional resistance, as shown in Figure 8. As a result, for the same BW dimension, the O-BW has a better effect in reducing wall deflection as compared to the I-BW, as indicated in Figure 5. However, for the case with ground anchors, their difference is insignificant, as indicated in Figure 6. This is because a very high flexural rigidity is established when the ground anchors are added, so the flexural rigidity provided by the combination of BW and DW had a more pronounced effect than the additional frictional resistance. This phenomenon is in agreement with the findings conducted by Hsieh and Ou (2018), where the flexural rigidity provided by the BW can effectively restrain the deformation of the DW when maintaining the BWs.

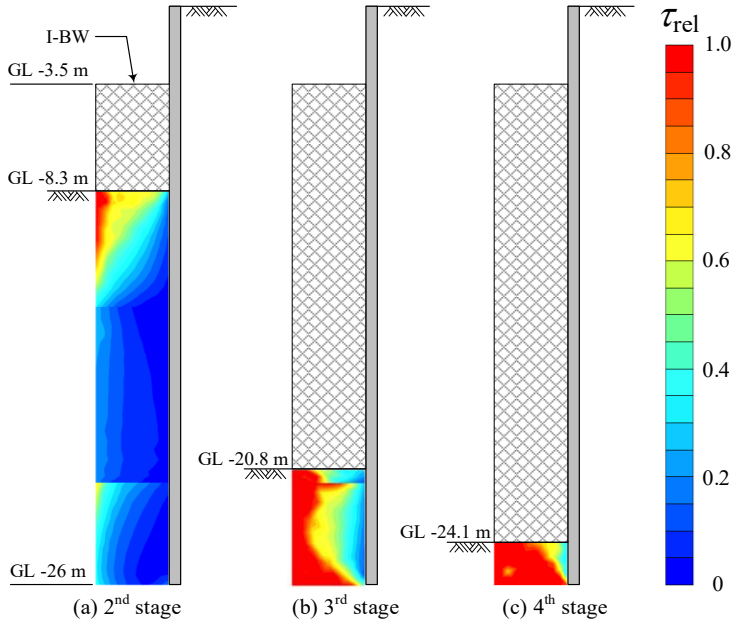

Figure 7. The relative shear stress distribution of the inner buttress wall (I-BW) at excavation stages

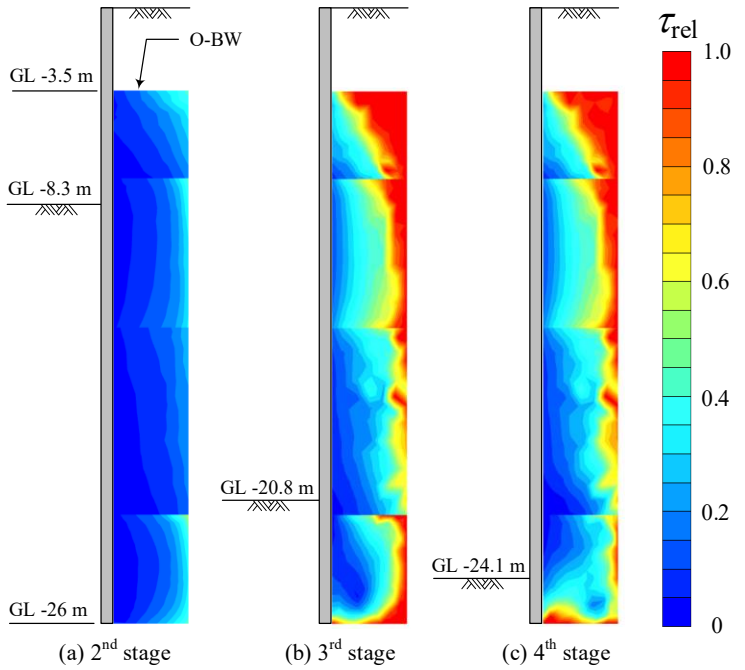

Figure 8. The relative shear stress distribution of the outer buttress wall (I-BW) at different excavation stages

Figure 9 presents the computed ground anchor forces for the two BW types (I-BW and O-BW) as well as without BW at the final excavation stage. The results showed that O-BW is slightly better than I-BW in reducing ground anchor force, particularly for the lowest ground anchor level (I-BW reduce anchor force by 9.38%, whereas O-BW reduce anchor force by 15.14%). Meanwhile, a larger ground anchor force is found at the lowest level for the case without BW as compared to the I-BW and O-BW cases. This is because the ground anchor is applied prior to the final excavation stage, so the highest impact of the ground anchor force for different BW conditions would occur at the lowest level. Finally, this finding further indicates that the BW is beneficial in reducing the ground anchor force at the final excavation stage, particularly at the lowest anchor level.

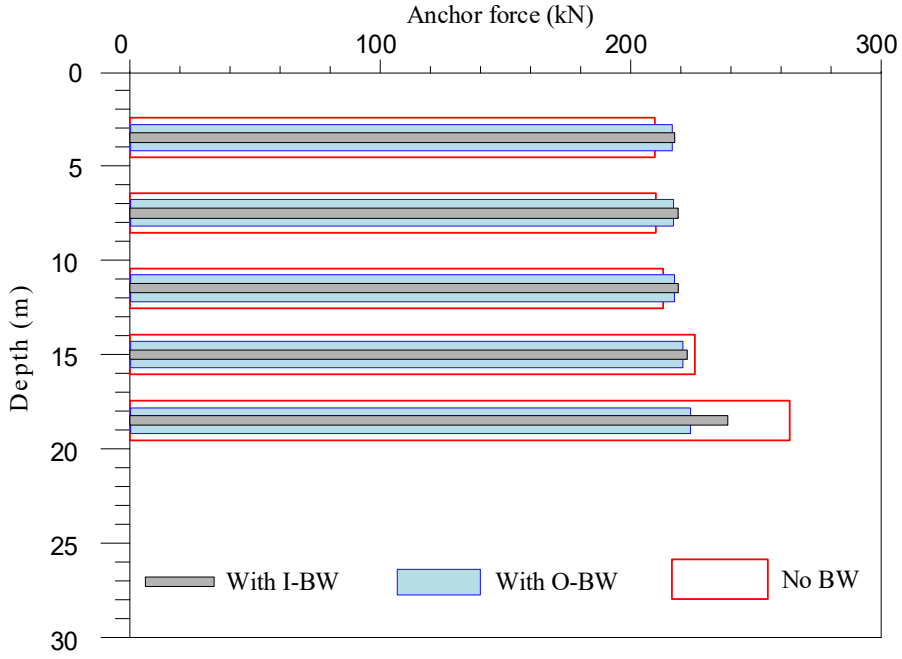

Figure 9. Computed anchor force at all levels for inner and outer buttress wall (I-BW and O-BW) at the final excavation stage.

5 CONCLUSIONS AND RECOMMENDATIONS

5.1 Conclusions

In this paper, the performance of buttress wall (BW) in reducing wall deflections and ground anchor forces for deep excavation with a tied-back wall system is evaluated through three-dimensional finite element method (3D FEM). A case history was initially utilized to validate the numerical analysis. Thereafter, parametric studies were performed to evaluate the performance of BW considering different BW configurations, with and without ground anchors. An additional analysis was conducted considering only ground anchors and without BW. According to the results obtained from the numerical analyses, the following conclusions can be drawn:

1. Both the computed wall deflections and field measurements generally exhibited good agreement across all excavation stages, displaying a similar characteristic linear cantilever profile.
2. When the BW was demolished after the final excavation stage, the wall deflection slightly increased, but the maximum wall deflection can still be controlled due to additional supports by the ground anchors. This indicates that the ground anchor could effectively support and control DW deflection during the BW demolition.
3. The combination of both ground anchors and BW could effectively reduce the wall deflections along the depth. Additionally, implementing BW could also reduce ground anchor force, particularly at the lowest anchor level, providing a safer excavation system.

4. For the case without ground anchors, the outer BW (BW implemented behind the wall) was more effective in reducing wall deflections compared to the inner BW (BW implemented inside the excavation). This was because the frictional area acting on the BW surface for outer BW remains the same for all excavation stages, while the frictional area provided by inner BW reduces along with excavation. However, for the case with ground anchors, their difference is insignificant in reducing wall deflection because when implementing ground anchors, a very stiff supporting system is established, so the flexural rigidity provided by the combination of BW and DW had a more pronounced effect than the additional frictional resistance acting on the BW surface.

5.2 Limitations and Recommendations

Although this paper has demonstrated the effectiveness of the buttress wall (BW) system in reducing wall deflection in deep excavations with tied-back wall configurations, several limitations remain in the current analysis. These limitations are outlined below, along with recommendations for future research.

1. This study employed a linear-elastic model for the structural components of the BW, DW, and ground anchors. However, under failure conditions, the retaining wall may experience yielding due to large bending moments. Therefore, future research is recommended to incorporate elastoplastic structural behavior to more accurately capture and simulate such phenomenon.
2. In this parametric study, the configurations considered for BW were only limited to the location of the BW (inner and outer BW). Hence, for future study, it is recommended to further explore the influence of BW spacing and dimension on limiting wall deflection.

DISCLAIMER

The authors declare no conflict of interest.

AVAILABILITY OF DATA AND MATERIALS

All data are available from the author.

REFERENCES

Abdi, A. S., & Ou, C. Y., 2022. A Study of the Failure Mechanism of Braced Excavations Using 3D Finite-Element Analysis. *International Journal of Geomechanics*, 22(7), pp. 1–14. https://doi.org/10.1061/(ASCE)GM.1943-5622.0002385

Abdi, A. S., & Ou, C. Y., 2023a. Numerical Study of the Effect of Ground Improvement on Basal Heave Stability for Deep Excavations in Normally Consolidated Clays. *Journal of Geotechnical and Geoenvironmental Engineering (ASCE)*, 149(7), pp. 1–11. https://doi.org/10.1061/JGGEFK.GTENG-11022

Abdi, A. S., & Ou, C. Y., 2023b. Numerical evaluation on the performance of deep excavation with the strut-free retaining system in clays. *10th European Conference on Numerical Methods in Geotechnical Engineering*.

Abdi, A. S., 2024. Evaluation of cross wall performance on restraining the wall displacement and resisting the basal heave in deep excavations. *Acta Geotechnica*, 19(6), pp. 4037–4053. https://doi.org/10.1007/s11440-023-02142-6

Abdi, A. S., Ou, C., & Teng, F., 2024. Computers and Geotechnics Effect of cross wall on the strut forces for braced excavations in clays. *Computers and Geotechnics*, 171, 106344. https://doi.org/10.1016/j.compgeo.2024.106344

Abdi, A. S., 2025. *Three-Dimensional Analysis of Buttress and Cross Walls on Controlling Wall Deformation Induced by Deep Excavation*. 25(8), pp. 1–16. https://doi.org/10.1061/IJGNAI.GMENG-10928

ACI, 1995. *Building code requirements for structural concrete*. Farmington Hills: ACI 318R-American Concrete Institute.

Bolton, M. D., 1986. The strength and dilatancy of sands. *Géotechnique*, 36(1), pp. 65–78. https://doi.org/10.1680/geot.1986.36.1.65

Brinkgreve, R. B. J., Kumarswamy, S., & Swolfs, W. M., 2021. *PLAXIS Reference Manual*.

Bryson, L. S., & Zapata-Medina, D. G., 2012. Method for Estimating System Stiffness for Excavation Support Walls. *Journal of Geotechnical and Geoenvironmental Engineering*, 138(9), pp. 1104–1115. https://doi.org/10.1061/(asce)gt.1943-5606.0000683

Bui, L. M., Wu, L., Do, M. N., Cheng, Y., & Dong, D. J., 2024. Buttress wall in limiting wall deformation caused by deep excavation: A case study for colluvial soil in Vietnam. *Archives of Civil Engineering*, pp. 477–492. https://doi.org/10.24425/ace.2024.149876

Calvello, M., & Finno, R. J., 2004. Selecting parameters to optimize in model calibration by inverse analysis. *Computers and Geotechnics*, 31(5), pp. 410–424. https://doi.org/10.1016/j.compgeo.2004.03.004

Finno, R. J., & Roboski, J. F., 2005. Three-Dimensional Responses of a Tied-Back Excavation through Clay. *Journal of Geotechnical and Geoenvironmental Engineering*, 131(3), pp. 273–282. https://doi.org/10.1061/(asce)1090-0241(2005)131:3(273)

Hsieh, P. G., & Ou, C. Y., 2018. Mechanism of buttress walls in restraining the wall deflection caused by deep excavation. *Tunnelling and Underground Space Technology*, 82, pp. 542–553. https://doi.org/10.1016/j.tust.2018.09.004

Hsieh, P. G., Ou, C. Y., & Hsieh, W. H., 2016. Efficiency of excavations with buttress walls in reducing the deflection of the diaphragm wall. *Acta Geotechnica*, 11(5), pp. 1087–1102. https://doi.org/10.1007/s11440-015-0416-6

Hsiung, B. C. B., Yang, K. H., Aila, W., & Ge, L., 2018. Evaluation of the wall deflections of a deep excavation in Central Jakarta using three-dimensional modeling. *Tunnelling and Underground Space Technology*, 72, pp. 84–96. https://doi.org/10.1016/j.tust.2017.11.013

Lim, A., Hsieh, P. G., & Ou, C. Y., 2016. Evaluation of buttress wall shapes to limit movements induced by deep excavation. *Computers and Geotechnics*, 78, pp. 155–170. https://doi.org/10.1016/j.compgeo.2016.05.012

Lim, A., Ou, C. Y., & Hsieh, P. G., 2018. Investigation of the integrated retaining system to limit deformations induced by deep excavation. *Acta Geotechnica*, 13(4), pp. 973–995. https://doi.org/10.1007/s11440-017-0613-6

Lim, A., Ou, C. Y., & Hsieh, P. G., 2020. A novel strut-free retaining wall system for deep excavation in soft clay: numerical study. *Acta Geotechnica*, 15(6), pp. 1557–1576. https://doi.org/10.1007/s11440-019-00851-5

Ou, C. Y., Lin, Y. L., & Hsieh, P. G., 2006. Case record of an excavation with cross walls and buttress walls. *Journal of GeoEngineering*, 1(2), pp. 79–87. https://doi.org/10.6310/jog.2006.1(2).4

Ou, C. Y., Teng, F., & Li, C. W., 2020. A simplified estimation of excavation-induced ground movements for adjacent building damage potential assessment. *Tunnelling and Underground Space Technology*, 106(April), 103561. https://doi.org/10.1016/j.tust.2020.103561

Schanz, T., Vermeer, P. A., & Bonnier, P. G., 1999. The hardening soil model: Formulation and verification. *Beyond 2000 in Computational Geotechnics - 10 Years of Plaxis*.

Schuster, M., Kung, G. T.-C., Juang, C. H., & Hashash, Y. M. A., 2009. Simplified Model for Evaluating Damage Potential of Buildings Adjacent to a Braced Excavation. *Journal of Geotechnical and Geoenvironmental Engineering*, 135(12), pp. 1823–1835. https://doi.org/10.1061/(asce)gt.1943-5606.0000161

Teng, F., Hsiung, B.-C. B., Prakasa, M. D. A., Yang, K.-H., Anthony, & Litanes, R., 2023. Simulations on time-dependent behaviour based on wall deflection of deep excavations in Jakarta. *Arabian Journal of Geosciences*, 16(8), p. 482. https://doi.org/10.1007/s12517-023-11597-6

Zheng, G., He, X., Zhou, H., Diao, Y., Li, Z., & Liu, X., 2022. Performance of inclined-vertical framed retaining wall for excavation in clay. *Tunnelling and Underground Space Technology*, 130. https://doi.org/10.1016/j.tust.2022.104767